RSC Advances

ROYAL SOCIETY OF CHEMISTRY

www.rsc.org/advances

Journal Name

RSC Publishing

ARTICLE

Simple route for gram synthesis of less defective few layered graphene and its electrochemical performance†

Cite this: DOI: 10.1039/x0xx00000x

Nazish Parveen, Mohd Omaish Ansari and Moo Hwan Cho*

Received 00th January 2012,
Accepted 00th January 2012

DOI: 10.1039/x0xx00000x

www.rsc.org/

The mass production of high-quality graphene (GN) sheets is essential for their practical applications on a large scale. This paper reports a simple and less corrosive technique for the electrochemical exfoliation of graphite sheets using an aqueous solution mixture of sodium hydroxide, sodium thiosulfate, and sodium hypochlorite ($NaOH+Na_2S_2O_3+NaClO_4$) as an electrolyte. The presence of $NaClO_4$ expanded the graphite lattice. NaOH in the electrolyte facilitated the electrochemical reduction of the preformed oxygen functional groups of GN while the sulphate ions of $Na_2S_2O_3$ accelerated the exfoliation of the graphite sheet. Along a series of chemical reactions, the oxidation process produced O_2 and SO_2 gases. These gases exerted additional forces on the graphite layers and separated the loosely bonded graphite layers, thereby accelerating the exfoliation process. The methodology produces large quantities of crystalline and high quality GN with few layered structures, and was thus called as few layered graphene (FLGN). The prepared FLGN was characterized using a range of techniques, including Raman spectroscopy and atomic force microscopy, which showed that the as-prepared graphene has 4-6 layers and a large lateral size, which was also confirmed by other analysis. The electrochemical properties of FLGN were examined by cyclic voltammetry, impedance spectroscopy and charge/discharge studies. The as-prepared FLGN exhibited a high specific capacity and good cyclic stability, which makes this methodology promising for the large scale production of FLGN for practical applications.

Introduction

Since the discovery of graphene (GN) by Novoselov in 2004, this unique material has attracted tremendous attention worldwide for its promising applications in various fields, such as electrical, electrochemical, supercapacitor, photochemical, optical, etc.[1,2] GN is comprised of sp^2-hybridized, single layered, two dimensional carbon atoms arranged in a honeycomb lattice.[3] The planer orbitals are energetically stable and localized sigma bonds with the three nearest neighbour atoms arranged in a honeycomb lattice. This structure of GN is responsible for its high surface area and electrical conductivity as well as its other exceptional properties.[4-6]

Many routes have been used for the synthesis of large surface area and high quality GN, including the mechanical exfoliation of graphite and chemical vapor deposition.[4,7] On the other hand, most of these methods suffer from a range of limitations, such as lower yield, agglomerated sheets, attached functional groups etc. Therefore, the synthesis of high quality few layered graphene sheet (FLGN) in larger amounts is a major challenge. The chemical method (Hummer's method) is an appealing route for the synthesis of reduced graphene oxide (RGO). This RGO is derived using different reducing agents; however, these RGO have various defects and are highly oxygenated with hydroxyl and epoxide functional groups, which limits their electrochemical applications because of their lower thermal conductivity.[7,8] Therefore, FLGN sheets with minimum functional groups (hydroxyl and epoxide) is desired from an applications point of view.

The electrochemical exfoliation of graphite sheets into GN using mild chemical processes without the need for a strong oxidizing agent has attracted attention because it is a simple, fast, low-cost, and environmental friendly method.[9,10] Yuan et al.[10] first reported this method for the synthesis of GN sheets in concentrated sulphuric acid in 2011. On the other hand, in the acidic medium, the honeycomb lattice of GN sheet sustained damage, such as defects and functionalization by various groups, during the exfoliation process, which may further limit its application. Owing to the corrosive nature of the oxidative environment, different routes involving basic media have attracted considerable attention. For FLGN synthesis, Zhou et al.[11] proposed the use of Na^+/dimethylsulfoxide complexes as intercalation agents and the subsequent addition of thionin acetate for exfoliation. These electrochemical exfoliation methods have numerous advantages, such as the easy processing of GN and functionalized GN. These methods, however, have major shortcomings, including the requirement of strong chemicals and hazardous reagents, such as ionic liquids, lithium perchlorate, phosphoric acid, and 3-(amino propyl) triethoxy silane, the extra steps involve high voltages which gives low quality, and multilayer GN formation. Therefore, a milder

less corrosive route for high quality GN sheets is needed for various application processes.

This paper reports the electrochemical exfoliation of graphite sheet via facile soft processing approach using the NaOH + $Na_2S_2O_3$ + $NaClO_4$ electrolyte system for the mass production of FLGN. In the electrolyte, the less corrosive medium of NaOH induces the electrochemical reduction of preformed oxygen functional groups of GN. A systematic study of the efficiency of the exfoliation process was conducted to determine the quality of the processed GN. These materials were characterized and used further as an electrode material in electrochemical experiments. In a 1M H_2SO_4 electrolyte solution, FLGN showed electrical double layer capacitance (EDLC) behavior according to cyclic voltammetry (CV), as well as enhanced capacitance and cyclic stability performance by the galvanostatic charge/discharge (GCD) measurements.

Experimental

Materials

Graphite sheets (10 x 1.5 x 0.5 cm^3) for the synthesis of the FLGNs were obtained from KOMAX, South Korea. Sodium hydroxide (NaOH), sodium hypochlorite ($NaClO_4$), sodium thiosulfate ($Na_2S_2O_3$), ethanol, and sulfuric acid (H_2SO_4) were purchased from Duksan Pure Chemicals, Co. Ltd. Korea. The water used in these experiments was de-ionized water obtained from a PURE ROUP 30 water purification system.

Methods

The microstructures of FLGN were examined by scanning electron microscopy (SEM, HITACHI-S4800), field emission transmission electron microscopy (FE-TEM, Tecnai G2 F20, FEI, USA) and atomic force microscopy (AFM, The Netherlands). The mean size of the flakes was calculated using Image J software. Phase analysis was performed by X-ray diffraction (XRD, PANalytical, X'Pert-PRO MPD, Netherland) using Cu Kα radiation (λ= 0.15405 nm). Raman spectroscopy was recorded on a Lab Ram HR 800 UV Raman microscope (Horiba Jobin-Yvon, France, λ = 514 nm) at the Gwangju Center, South Korea. The functional groups of FLGN and their interactions were examined by Fourier transform infrared (FTIR, Excalibur series FTS 3000 Bio-Rad spectrometer) spectroscopy. The optical properties of FLGN were analyzed by ultraviolet-visible-near infrared (UV-VIS-NIR, Cary 5000, VARIAN, USA) spectroscopy. The chemical state and surface composition was analyzed by X-ray photoelectron spectroscopy (XPS, ESCALAB 250 XPS system, Thermo Fisher Scientific, UK) using a monochromatized l Kα x-ray source (hν = 1486.6 eV). Electrochemical studies, such as CV, GCD and EIS were carried out using a potentiostat (Versa STAT 3, Princeton Research, USA).

Electrochemical synthesis of FLGN

Graphite flakes as an anode electrode and Pt wire as a cathode were used in the working cell for the electrochemical exfoliation of graphite. The electrolytic solution used in the exfoliation process consisted of 1M $Na_2S_2O_3$ + 0.5M $NaClO_4$ + 0.5M NaOH dissolved in 1 litre H_2O. The distance between the graphite and Pt electrode was kept to ~2 cm throughout the electrochemical process. Electrochemical exfoliation was carried out by applying a positive voltage (10 V) to the graphite electrode. Immediately after the reaction commenced, the solution gradually turned grey and then finally to an intense black (Fig. S1). The graphite anode dissociated constantly into flaky GN and exfoliated graphite sheet throughout the course of the reaction, which settled at the bottom of the bottle. After 3 hrs, the electrolyte solution containing the exfoliated graphite sheets were placed in an ultrasonic bath for 48 hrs, and the dispersion under ultrasonication was then filtered under suction, washed with excess water and ethanol to remove the impurities. Therefore, the prepared FLGN was heated to 80 ℃ for 6h and stored in a desiccator for further experiments. The amount of FLGN flakes was calculated to be 1.5 g.

Electrochemical measurements

All electrochemical measurements were performed with a potentiostat Versa STAT 3, Princeton Research, USA. The working electrode was prepared by casting a nafion-impregnated sample on a carbon paper electrode with a surface area of 1 cm^2. Typically, 5 mg of FLGN was dispersed in 1 mL of an ethanol solution containing 5 μL of a nafion solution in an ultrasonic bath for 20 min, which was then coated on carbon paper. A three electrode cell system was used to evaluate the electrochemical performance, i.e. CV, EIS and GCD in the 1M H_2SO_4 electrolyte. FLGN coated carbon paper, Pt gauze and AgCl/Ag were used as the working, counter and reference electrodes, respectively, during the electrochemical process.

From the CV, the specific capacitance (C_{sp}) of the electrodes was determined using the following equation:

$$C_{sp} = 2[I/\text{Scan Rate } (dv/dt)VM] \quad (1)$$

where I is the average current during the cathodic and anodic sweep, V is the potential and M is the weight of active material coated on the carbon paper electrode.

From the GCD data recorded at a selected current density, the C_{sp} of the electrodes was determined using the following equation:

$$C_{sp} = 2\ (I\ dt\ /mdv) \quad (2)$$

where I, dv, dt, and m is the constant current used for charging discharging, voltage difference, discharge time, and the weight of the active electrode material coated on the carbon paper electrode, respectively.

Results and discussion

Proposed mechanism of electrochemical exfoliation of graphite sheet into graphene

The synthesis of GN through the electrochemical exfoliation of graphite has mainly been performed using acid electrolytes, such as H_2SO_4, H_3PO_4 and ionic liquid electrolyte.[12,13] On the other hand, the ionic liquids and acid electrolyte have been reported to cause many defects and oxidation, which can damage the honeycomb lattice of GN, resulting in GN flakes with inferior quality.[13,14] Schniep et al.[15] reported that an acid treatment of graphite results in

surface functionalization, such as epoxidation, which may greatly alter the properties of GN. Although most of the functional groups can be removed by chemical or thermal reduction, a significant number of framework defects and small defective GN fragments will exist and disrupt the desirable electronic properties.[16,14] To minimize the defects induced due to the corrosive acidic environment, an electrochemical exfoliation methodology of graphite under a basic medium has been proposed. Fig. 1 presents a schematic representation of the synthesis process.

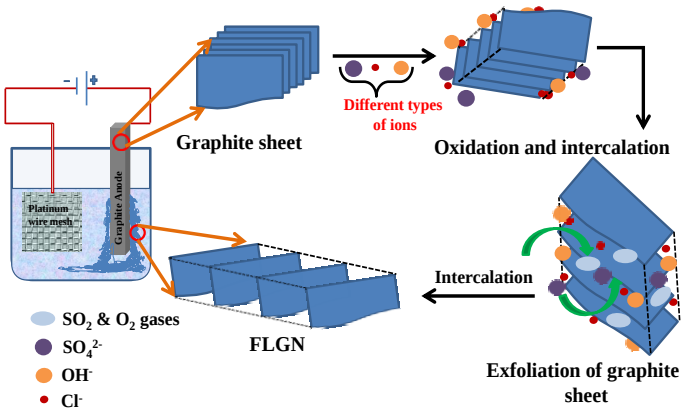

Fig. 1 Schematic diagram of the mechanism of electrochemical exfoliation of FLGN.

Parvez et al.[17] reported that a salt containing $NaClO_4$ expands the graphite lattice, which might be helpful in the exfoliation process. In the present case, 1M $NaClO_4$ in the electrolytic solution was used; however, no significant exfoliation of graphite sheets was observed. Another basic media containing 1M NaOH was also studied, but poor exfoliation occurred with very small yield. Therefore, it can be concluded that $NaClO_4$ and NaOH can affect the exfoliation process, of which NaOH shows better efficiency. As the $NaClO_4$ and NaOH system is expected to provide low exfoliation efficiency, a further modification to the electrolytic system was needed. Sulphate ions have been reported to accelerate the exfoliation of graphite, producing highly dispersed GN flakes.[12] The superior exfoliation efficiency of sulphate salts compared to other anions can be attributed to the lower reduction potential of SO_4^{2-} to generate SO_2 gas,[18] which is believed to accelerate the exfoliation process. Therefore, in the present study, a unique system of NaOH+$NaClO_4$+$Na_2S_2O_3$ was used for the synthesis of FLGN (Table S1 briefs the experimental conditions and the observed results during the exfoliation process). The electrolytic solution examined in the electrochemical exfoliation process consisted of $Na_2S_2O_3$, inorganic $NaClO_4$ and NaOH, as stated above. As soon as the voltage was passed, a mixture of GN sheets, exfoliated graphite sheets with loosely attached layers as well as unexfoliated graphite sheet were obtained readily within 5 min which settled at the bottom of the electrolytic cell as is seen in Fig S1. Two control experiments were also performed in the presence of NaOH+$Na_2S_2O_3$ and $Na_2S_2O_3$+$NaClO_4$ electrolyte. In both the experiments, very slow exfoliation was observed due to the formation of precipitate in the electrolytic solution which covered the graphitic electrode. These experiments conformed that the combination of NaOH+$NaClO_4$+$Na_2S_2O_3$ electrolyte works best for the exfoliation of graphite. The exfoliation mechanism can be understood by the synergistic effects of the various ions used in the electrolytic cell system.

a) In the electrolytic cell, due to the dissociation process, the aqueous solution of NaOH, $NaClO_4$ and $Na_2S_2O_3$ consists of Na^+, Cl^-, H^+, HO^-, and SO_4^{2-} ions in the electrolyte and can intercalate into the graphite sheets, thereby exfoliating the graphite sheet into GN layers.

b) As soon as the voltage is applied, the water molecules are reduced at the cathode, producing OH^- ions that act as a strong nucleophile in the electrolyte.[19]

c) All the ionic species as well as the formed OH^- ions, attacked at the edge sites and grain boundaries of the graphite sheet,[16] which accelerated the exfoliation process.

d) Another favorable reaction taking place is the self-oxidation of water and other oxidation processes taking place in the system producing gases, such as O_2, SO_2 etc.[20] These gases apply large forces to the graphite layers, which also helps to separate the loosely bonded graphite layers.

FTIR and UV-vis diffuse absorption analysis

FTIR analysis was performed to examine the chemical structure and any possible functional groups present in the as synthesized FLGN (Fig. 2a). In the present case, FLGN showed a band at 1578 cm^{-1} due to the C=C bond stretching while the broad band at 1344 and 1377 cm^{-1} was assigned to the C-H bending. Therefore, the FTIR peaks of the as-synthesized FLGN matches well with previously published reports, confirming its successful synthesis.[21,22] On the other hand, an additional peak was also observed at 1448 and 1100 cm^{-1}, which is due to CO-H bending and C-O stretching, respectively, suggesting that a small quantity of oxygen functional groups was introduced into FLGN during the exfoliation process.

Fig. 2b shows the UV-vis diffuse absorption spectra of FLGN. Only a single absorption peak centered at 251 nm, corresponding to the C=C bonds, was observed, suggesting that the as-synthesized FLGN did not have any other prominent functional groups.[23,27]

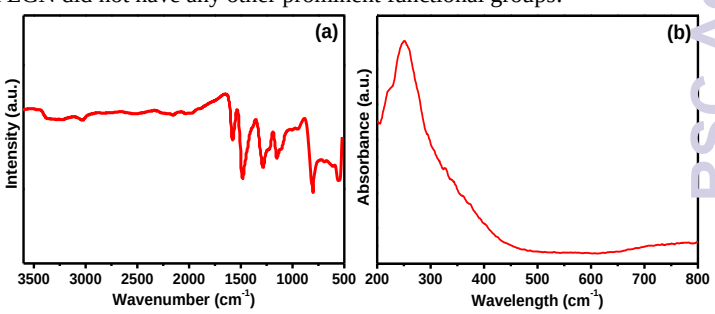

Fig. 2 (**a**) FTIR spectra and (**b**) UV-vis absorption spectra of FLGN.

Raman spectroscopy

Raman spectroscopy is one of the most successful tools for investigating the electronic/structural properties as well as for relating the defects in GN. The Raman spectrum of the as-

synthesized FLGN consisted of three major regions, i.e. the D, G and 2D bands (Fig. 3). The D band at 1353 cm^{-1} was assigned to the breathing mode of the sp^2 carbon atom, which was activated by the presence of small amount of defects.[24] The G band at 1583 cm^{-1} originates from stokes Raman scattering with one phonon (E_{2g}) emission. The I_D/I_G ratio is related to the number of defect/disordered carbon structures. The Raman spectra was analysed at 4 different place of FLGN and the I_D/I_G and I_G/I_{2D} ratio was calculated to quantify the amount of defects and quality of the FLGN (Fig. S2). The I_D/I_G = 0.35 obtained in the present case indicates the presence of very small percentage of defects in the GN sheet.[23,25] When correlated with the FTIR results, it can be concluded that during the exfoliation process, few oxygen functional groups are introduced in the FLGN, which also causes partial disorder at the carbon edges, and might be related to the defects present. Other similar reports on chemically reduced GO in an acidic electrolyte revealed a much higher I_D/I_G ratio of 0.4,[26] which highlights the efficacy of the proposed method of preparation.[11] The other band, i.e., 2D band, is excited by a double-resonant Raman process. The 2D band at 2691 cm^{-1} and the intensity ratio, $I_G/2I_D$ = 2.1, confirmed that the electrochemically exfoliated graphite sheet had only a few layers.[23,27] This is also supported by the broadening of the 2D band (inset of Fig. 3).

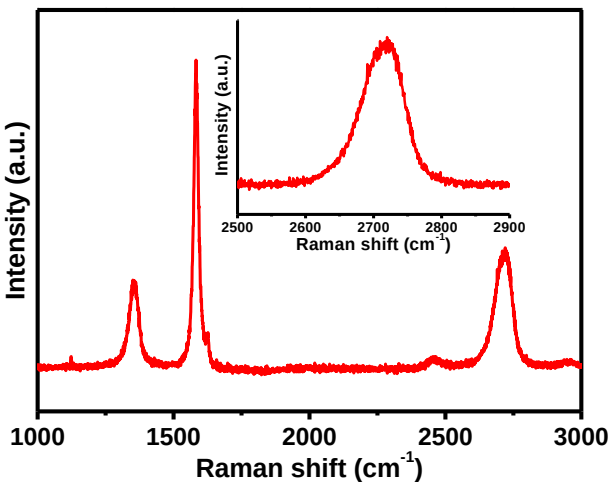

Fig. 3 Raman spectrum of FLGN.

SEM analysis

SEM and AFM were performed to study the surface features of the FLGN. SEM of FLGN was performed after dispersing it in ethanol by ultra-sonication and subsequently dropping it onto a silicon wafer for imaging. The inter-sheet spacing can be clearly seen from the image (Fig. 4a), suggesting a high level of exfoliation. The SEM image (Fig. 4b and 4c) of FLGN revealed wrinkled flake-like morphology with well-arranged staked sheets.[11,27] The well-ordered arrangement of the sheets obtained here was attributed to the less corrosive basic medium used, which is in contrast to the generally used acidic corrosive medium for the exfoliation process. From Image J software the calculated mean lateral size of the FLGN flakes was obtained to be ~4µm.

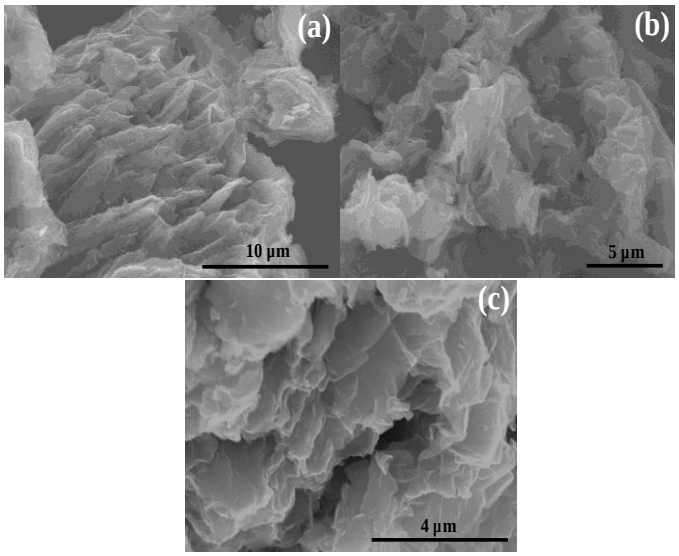

Fig. 4 SEM images of FLGN at different magnifications.

AFM analysis

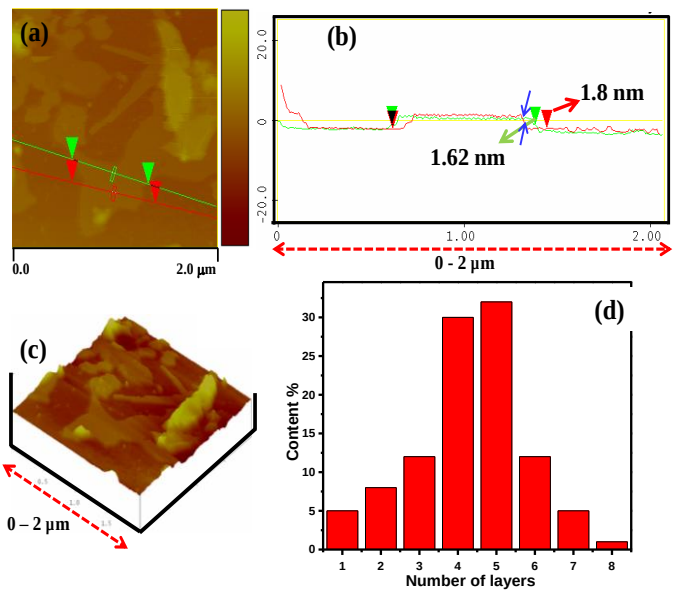

Fig. 5 (a-c) AFM image and (**d**) statistical thickness histogram of the electrochemically exfoliated FLGN.

The AFM image was used to measure the dimensions and thickness of the isolated FLGN. Fig. 5 and S3 show typical AFM image of the electrochemically exfoliated as synthesized FLGN which was randomly deposited on the silicon substrate. A smooth FLGN was selected for further investigation by the three-dimensional (3D) view. The GN surface was rough on the nanoscopic scale with some wrinkles, which may be due to the existence of functional groups as evident from the FTIR analysis. Limitation of the technique arising from the relatively large curvature radius of the AFM tip, the actual thickness of the graphene

sheet was difficult to measure with any accuracy. The thickness of the FLGN agglomerates was measured from several surface profiles using tapping mode AFM and the mean thickness was ~1.34 to 1.9 nm. This range is typical for 4-5 layers GN and is also supported by the observations reported by Andia et al.[23] for their GN sheets synthesized for high temperature applications.

In Fig. 5d, the statistical thickness analysis for the roughly 150 GN sheet from the AFM height profile ensemble shows that all of the GN sheets had a thickness lower than 3 nm and more than 50% of the sheets were thinner than 2 nm. Besides AFM, Raman and HRTEM are also confirming that the exfoliated GN was 4-5 layered.

TEM analysis

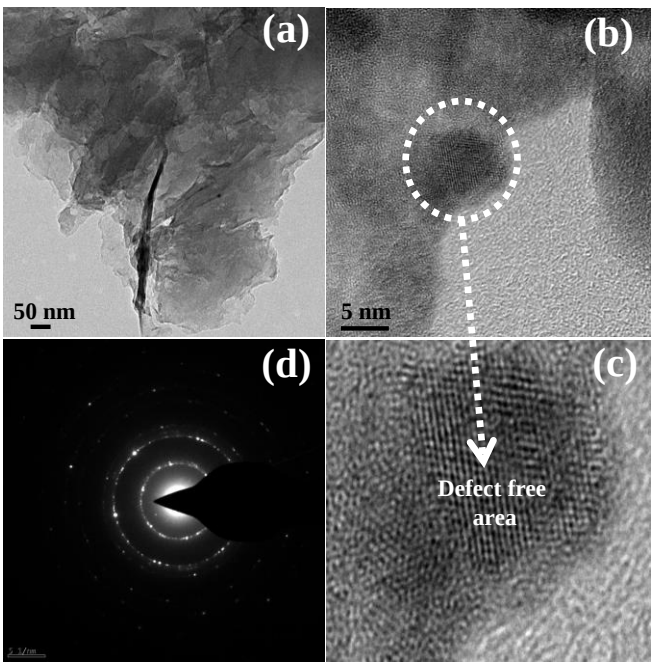

Fig. 6 (**a**) TEM, (**b** and **c**) HR-TEM image, and (**d**) SAED pattern of FLGN.

Fig. 6 and S4 showed the TEM and high resolution transmission electron microscopy (HR-TEM) images of the as-synthesized FLGN. A homogeneous wrinkled film like arrangement can be seen clearly at lower magnifications (Fig. 6a and S5). The HR-TEM image (Fig. 6b and S5) showed that the as-synthesized FLGN has a largely uniform lattice arrangement, but areas with some defects are also present. The selected defect free area of HR-TEM (Fig. 6b, 6c, S5a, S5b and S5c) revealed a highly uniform ordered arrangement, indicating the presence of a large π-network. The observed hexagonal carbon lattice patterns of the selective area electron diffraction (SAED) revealed the presence of sp^2-bonded carbon frameworks. In SAED pattern (Fig. 6d) of FLGN has some dots appeared due to the layered structure (4-5 layers) and presence of small defects. A systematic investigation on the statistical distribution of the FLGN layers was conducted through an examination of HR-TEM images. The measured lattice spacing of ~0.35 nm is consistent with that reported in the literature (Fig. S5a and S5b).[28] This indicates the insertion of fewer oxygen functional groups during the exfoliation process, which is also consistent with FTIR and Raman spectroscopy.

XPS and XRD analysis

XPS was performed to determine the surface characterization, chemical composition i.e. types of carbon and oxygen bonds, as well as the percentage of oxygen present in the as-synthesized FLGN. The wide-scan XPS spectrum of FLGN (Fig. S6) consisted largely of carbon (96.52%) and a small amount of functionalized oxygen (3.48%), which correlates well with the FTIR and Raman analysis. These results confirming that the as synthesised FLGN is largely free from defects. Liu et al.[29] reported an oxygen percentage of 16.3% in their FLGN. In contrast, the functionalization of oxygen was much lower in the present case, which indicates the efficacy of the preparation method.

To further determinate the chemical bond state of carbon in the FLGN the C1s core level was examined. The C 1s of XPS spectrum (Fig. 7) was confirms that a very small amount of oxygen functional groups (3.48%) had been introduced during the exfoliation of graphite into FLGN. The bands corresponding to C-C (284.98), C−OH (285.58 eV) and C=O (287.6 eV) were consistent with the literature.[30]

Fig. S7 presents the XRD patterns of FLGN and graphite sheet. The values of d_{002} were calculated using Bragg's equation ($n\lambda = 2d\sin\theta$, where n = 1, λ is the wave length, 1.5406 Å). A more intense 002 peak in the case of FLGN was observed at 26.45 (d-spacing ~3.41) whereas it was observed at 26.61 (d-spacing ~3.34) for the graphite sheet. These results are in accordance with the reports by Parvez at al.[17] for their exfoliated graphite by the inorganic salt medium. The shifting of the diffraction angle of FLGN to a lower 2θ value, suggested the possible expansion of the hexagonal lattice ring of graphite during the exfoliation process.

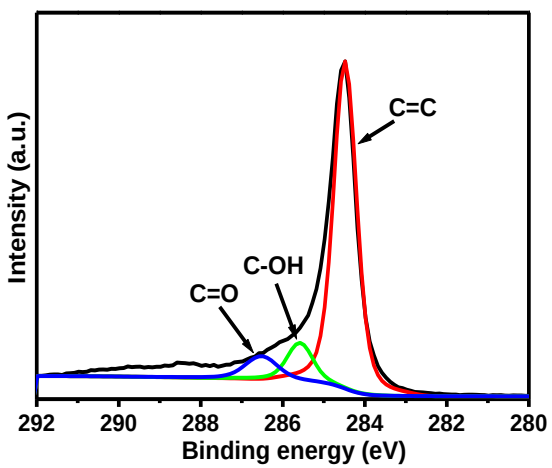

Fig. 7 C 1s spectra of FLGN.

Electrochemical studies

Cyclic voltammetry

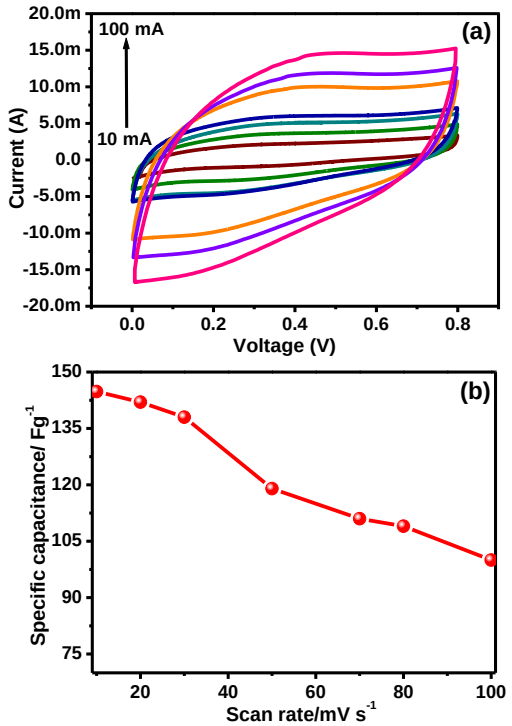

Fig. 8 (**a**) Cyclic voltammograms with different scan rates and (**b**) specific capacitance of FLGN.

CV is generally used for examining the capacitive properties, redox nature and charge/discharge behavior of the materials. In the case of the as-prepared FLGN, the measurements were performed at room temperature within the potential range of 0 to 0.8 V and at scan rates of 10 to 100 mV/s. The shape of the CV curve of FLGN, as evident from Fig. 8a, is more or less rectangular in shape. The presence of a redox peak is due to the additional functional groups, which can interact with the protons from the acidic medium. In the light of other's reports[31], the rectangular CV curves obtained in the present case represents the high electrochemical performances in electric double layer capacitors (EDLCs), which is associated with the rapid response of the current to the voltage reversal.[31] The capacitance of the FLGN electrode was calculated from the cyclic voltammograms (Fig. 8b), recorded at different scan rates using equation 1. The voltammograms in Fig. 8a did not show any redox peak, which suggests that the capacitive behaviour is free from various types of redox reactions.[32,33] The non-observance of a redox peak was noted at all scan rates up to 100 mV/s, suggesting high capacitive behaviour over a wide range of scan rates. The maximum specific capacitance of FLGN 147 F/g at a current density 10 mV/s, which is much higher than previously reported papers, and are summarized in Table S2.[34,35,36]

Fig. 8b shows the capacitance values determined using equation (1) and the voltammograms obtained at different scan rates. As the scan rate was increased above 10 mV/s the voltammograms 'window' tended to tilt towards the vertical axis. This highlights the dominance of the double layer formation in the energy storage process at lower scan rates. From Fig. 8b, it can also be seen that FLGN shows decreasing capacitance with increasing scan rates. FLGN showed a specific capacitance of ~147 F/g at a scan rate of 10mV/s but the capacitance value decreased to ~100 F/g at 100mV/s. It can be concluded that for very low scan rates, the capacitance is generally higher because the ions have a much longer time to enter and exist in the available electrode pores to form electric double layers, which are needed to generate higher capacitance.

Galvanostatic charge-discharge

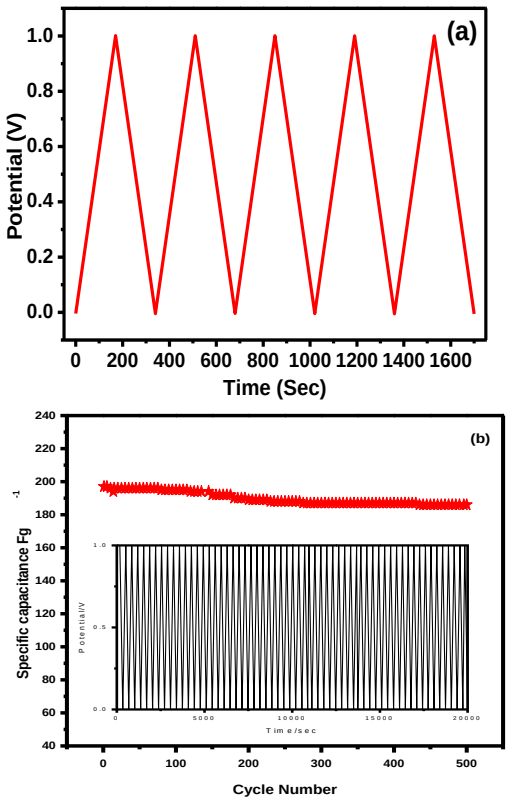

Fig. 9 (**a**) Galvanostatic charge discharge measurement at 0-1voltage range and (**b**) cyclic stability of FLGN.

The GCD curve of FLGN was recorded over the potential range of 0-1 V and at a current density of 10 mA (Fig. 9a). All the curves showed a similar symmetrical triangular and there was no large IR drop with a linear variation of voltage as a function of time during the charge and discharge process. Therefore, the type of curve obtained in the present case of FLGN is typical for a carbon-based supercapacitor, and the data shows that FLGN exhibits good capacitive performance.[37,38] The capacitance values of the FLGN electrodes were calculated to be 197 Ag^{-1} at 10 mA from Fig. 9a using equation (2) which is much higher than previously reported electrochemically exfoliated GN.[29] On the other hand, in the cyclic stability test of FLGN, despite having a similar shape of the curve, it showed significantly higher charge and discharge times, indicating that a larger number of electrons and electrolyte ions contribute to the charge and discharge processes.[39,40] The long-term cycling stability of the FLGN was also confirmed by the cyclic

charge/discharge process at a fixed current density of 10 mA/cm^2, as shown Fig. 9b. The FLGN remained at 97% of the capacitance after 500 charge/discharge cycles, highlighting its excellent long-term cycling stability, which is also similar to the previously reported GN.[36] The inset in the Fig. 9b showed no significant electrochemical change during the long-term charging and discharging process after 500 cycles.

Electrochemical impedance spectroscopy

EIS is an important analytical technique used to obtain information on the characteristic frequency responses of supercapacitors and the capacitive phenomenon occurring in the electrodes. The Nyquist plots generally show the frequency response of the electrode/electrolyte system and are a plot of the imaginary component (Z'') as a function of the real component (Z'). Each data point is set at a different frequency with the lower portion of the curve corresponding to the higher frequency. EIS was performed over a range of frequencies (1-104 Hz) and a potential of 0.5V using Nyquist plots. In Fig. 10, the Nyquist plot of FLGN electrodes showed a straight line in the low-frequency region and a small semicircle in the high frequency region. At high frequencies, the resistance characteristics of the different supercapacitors are expressed as the equivalent series resistance (ESR), which includes the electrolyte resistance, the collector/electrode contact resistance and the electrode/electrolyte interface resistance. The intersection of the curve with the X-axis shows that the internal or equivalent series resistance is a key parameter influencing the charge/discharge rate, as a smaller ESR value represents a lesser internal loss and a greater charge/discharge rate.[41,42] The ESR of the carbon electrodes was higher because it has attached more surface functional groups, which decrease the electronic conductivity of the material.[39] As shown in the curve, the ESR value of FLGN was very small, indicating a decreased internal resistance. The vertical shape at lower frequencies indicates pure capacitive behavior, which is representative of ion diffusion in the electrode structure.

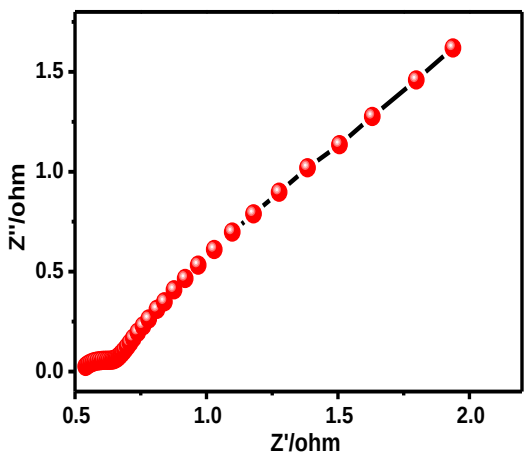

Fig. 10 EIS Nyquist plot of FLGN.

Conclusions

In this study, a simple electrochemical exfoliation route was developed for the rapid production of FLGN. The proposed methodology has a number of advantages over reported methods owing to its simple reaction set up, environmentally-friendly/less corrosive route, single-step synthesis, and highly effective exfoliation of graphite sheets. The exfoliation process showed reduced oxidation degree with 96.52% of carbon and only 3.48% of functionalized oxygen, hence confirming that the as synthesised FLGN is largely free of any defects and possess much ordered Owing to this, there is high uniformly of π-π interaction in the as synthesised FLGN which gives high electrochemical results. The CV studies showed that FLGN exhibited an EDLC nature and the capacitance decreased with increasing scan rate. Similarly, GCD also showed enhanced capacitance and good cyclic stability. Owing to the high capacitance and high stability, the as-synthesized FLGN is expected to act as a replacement electrode material for applications in supercapacitors and electronic devices.

Acknowledgements

This study was supported by Priority Research Centers Program through the National Research Foundation of Korea (NRF) funded by the Ministry of Education (2014R1A6A1031189).

Notes and references

School of Chemical Engineering, Yeungnam University, Gyeongsan-si, Gyeongbuk 712-749, South Korea. Phone: +82-53-810-2517; Fax: +82-53-810-463.
***Corresponding author Email:** mhcho@ynu.ac.kr*

†Electronic Supplementary Information (ESI) available: [Digital photographs of gram synthesis of FLGN, I_D/I_G and I_G/I_{2D} ratio bar graph, AFM image of FLGN, TEM image of FLGN, HR-TEM images of FLGN, XPS survey spectra of FLGN, XRD pattern of FLGN and Table S1 and S2] See DOI: 10.1039/b000000x/

1 X. Dong, C.Y. Su, W. Zhang, J. Zhao, Q. Ling, W. Huang, P. Chen and L.J. Li, *Phys. Chem. Chem. Phys.*, 2010, **12**, 2164–2169.
2 H. Liu, S. Ryu, Z. Chen, M. L. Steigerwald, C. Nuckolls and L. E. Brus, *J. Am. Chem. Soc.*, 2009, **131**, 17099–17101.
3 Q. Zheng, B. Zhang, X. Lin, X. Shen, N. Yousefi, Z.D. Huang, Z. Li and J.K. Kim, *J. Mater. Chem.*, 2012, **22**, 25072–25082.
4 S. B. Jo, J. Park, W. H. Lee, K. Cho and B. H. Hong, *Solid State Commun.*, 2012, **152**, 1350–1358.
5 K. Yadav, H. J. Yoo, J. W. Cho, *Journal of Polymer Science Part B: Polymer Physics*, 2013, **51**, 39–47.
6 Z. Khan, T. R. Chetia, A. K. Vardhaman, D. Barpuzary, C.V. Sastri and M. Qureshi, *RSC Adv.*, 2012, **2**, 12122–12128.
7 B. K. Barman and K. K. Nanda, *RSC Adv.*, 2014, **4**, 44146–44150.
8 X. Dong, W. Huang and P. Chen, *Nanoscale Res. Lett.*, 2011, 6:60, 1−6.

9 J. Liu, M. Notarianni, G. Will, V. T. Tiong, H. Wang, and N. Motta, *Langmuir*, 2013, **29**, 13307−13314.
10 C. Y. Su, A. Y. Lu, Y. Xu, F. R. Chen, A. N. Khlobystov and L. J. Li, *ACS Nano*, 5, 2332–2339.
11 M. Zhou, J. Tang, Q. Cheng, G. Xu, P. Cui and L. C. Qin, *Chem. Phy. Lett.*, 2013, **572**, 61–65.
12 L. Buglione, E. L. K. Chng, A. Ambrosi, Z. Sofer, M. Pumera, *Electrochem. Commun.*, 2012, **14**, 5–8.
13 N. Liu, F. Luo, H. Wu, Y. Liu, C. Zhang, and J. Chen, *Adv. Funct. Mater.*, 2008, **18**, 1518–1525.
14 N. G. Shang, P. Papakonstantinou, S. Sharma, G. Lubarsky, M. Li, D. W. M. Neill, A J. Quinn, W. Zhoue and R. Blackley, *Chem. Commun.*, 2012, **48**, 1877–1879.
15 H. C. Schniepp, J. L. Li, M. J. McAllister, H. Sai, M. H. Alonso, D. H. Adamson, R. K. Prudhomme, R. Car, D. A. Saville, and I. A. Aksay, *J. Phys. Chem. B*, 2006, **110**, 8535–8539.
16 C. G. Navarro, J. C. Meyer, R. S. Sundaram, A. Chuvilin, S. Kurasch, M. Burghard, K. Kern, and U. Kaiser, *Nano Lett.*, 2010, **10**, 1144–1148.
17 K. Parvez, Z. S. Wu, R. Li, X. Liu, R. Graf, X. Feng, and K. Mullen, *J. Am. Chem. Soc.*, 2014, **136**, 6083−6091.
18 F. Bech, H. Junge and H. Krohn, *Electrochim. Acta*, 1981, **26** 799–809.
19 N. J. Bunce, D. Bejan, *Electrochim. Acta*, 2011, **56**, 8085–8093.
20 F. Beck, J. Jiang and H. Krohn, *J. Electroanal. Chem.*, 1995, **389**, 161−165.
21 R. Kumar, P. Kumar, S. Naqvi,a N. Gupta, N. Saxena, J. Gaur, J. K. Mauryac and S. Chand, *New J. Chem.*, 2014, **38**, 4922−4930.
22 H. Li, T. Lu, L. Pan, Y. Zhang and Z. Sun, *J. Mater. Chem.*, 2009, **19**, 6773–6779.
23 P. M. Andia, F. Simon, G. Heinrich and K. K. Nanda, *Chem. Commun.*, 2014, **50**, 4613−4615.
24 A. C. Ferrari, J. C. Meyer, V. Scardaci, C. Casiraghi, M. Lazzeri, F. Mauri, S. Piscanec, D. Jiang, K. S. Novoselov, S. Roth and A. K. Geim, *Phys. Rev. Lett.*, 2006, **97**, 187401–4.
25 L. G. Cancado, A. Jorio, E. H. M. Ferreira, F. Stavale, C. A. Achete, R. B. Capaz, M. V. O. Moutinho, A. Lombardo, T. S. Kulmala and A. C. Ferrari, *Nano Lett.*, 2011, **11**, 3190–3196.
26 K. Parvez, R. Li, S. R. Puniredd, Y. Hernandez, F. Hinkel, S. Wang, X. Feng and K. Mullen, *ACS Nano*, 2013, **7**, 3598–3606.
27 D. Nuvoli, L. Valentini, V. Alzari, S. Scognamillo, S. B. Bon, M. Piccinini, J. Illescasd and A. Mariani, *J. Mater. Chem.*, 2011, **21**, 3428–3431.
28 H. Ham, N. H. Park, I. Kang, H W. Kim and K. B. Shim, *Chem. Commun.*, 2012, **48**, 6672–6674.
29 J. Liu, M. Notarianni, G. Will, V. T. Tiong, H. Wang, and N. Motta, *Langmuir*, 2013, **29**, 13307−13314.
30 S. Park, J. An, R. D. Piner, I. Jung, D. Yang, A. Vmakanni, S. T. Nguyen, and R. S. Ruoff, *Chem. Mater.*, 2008, **20**, 6592–6594.
31 L. Dong, C. Xu, Q. Yang, J. Fang, Y. Lic and F Kang, J. Mater. Chem. A, 2015, **3**, 4729–4737.
32 J. Yan, Z. Fan, T. Wei, W. Qian, M. Zhang and F. Wei, *Carbon*, 2010, **48**, 3825–3833.
33 A.I. Inamdar , Y. Kima, S.M. Pawar , J.H. Kimb, H. Ima, H. Kim, *J. Power Sources*, 2011, **196**, 2393–2397.
34 S. R. C. Vivekchand, C.S. ROUT, K. S. Subrahmanyam, and C N R Rao, J. Chem. Sci., 2008, 120, 9–13.
35 Y. Li, M. Zijll, S. Chiang, N. Pan, Journal of Power Sources, 2011, 196, 6003–6006.
36 G. Wang, X. Sun, F. Lu, H. Sun, M. Yu, W. Jiang, C. Liu and J. Lian, Nano small., 2012, 3, 452–459.
37 G. Z. Chen, *Prog. Nat. Sci.*, 2013, **23**, 245–255.
38 J. Zang, C. Cao, Y. Feng, J. Liu, X. Zhao, *Sci. Rep.*, 2014, **4**, 6492 (1-7).
39 B. Subramanya and D. K. Bhat, *New J. Chem.*, 2015, **39**, 420–430.
40 R. Vellacheri, A. Al-Haddad, H. Zhao, W. Wang, C. Wang and Y. Lei, *Nano Energy*, 2014, **8**, 231–237.
41 D. Zhang, X. Wen, L. Shi, T. Yana and J. Zhang, *Nanoscale*, 2012, **4**, 5440–5446.
42 H. Wei, S. Wei, W. Tian, D. Zhu, Y. Liu, L. Yuan and X. Li, *Sci. Rep.*, 2014, **4**, 7050 (1-9).

